Supplemental Material for "Microwave Quantum Illumination"

Shabir Barzanjeh,[1] Saikat Guha,[2] Christian Weedbrook,[3] David Vitali,[4] Jeffrey H. Shapiro,[5] and Stefano Pirandola[6]

[1] *Institute for Quantum Information, RWTH Aachen University, 52056 Aachen, Germany*
[2] *Quantum Information Processing Group, Raytheon BBN Technologies, Cambridge, Massachusetts 02138, USA*
[3] *QKD Corp., 60 St. George St., Toronto, M5S 3G4, Canada*
[4] *School of Science and Technology, University of Camerino, Camerino, Macerata 62032, Italy*
[5] *Research Laboratory of Electronics, Massachusetts Institute of Technology, Cambridge, Massachusetts 02139, USA*
[6] *Department of Computer Science & York Centre for Quantum Technologies, University of York, York YO10 5GH, United Kingdom*

In this Supplemental Material we provide technical details on the following: (i) Hamiltonian of an electro-opto-mechanical system, (ii) linearization of the Hamiltonian, (iii) derivation of the quantum Langevin equations with internal losses, (iv) study of the microwave-optical entanglement considering the entanglement metric, the logarithmic negativity and the coherent information, (v) general study of the quantum correlations as quantified by quantum discord, and (vi) analysis of the error probability for M mode pairs.

I. HAMILTONIAN OF AN ELECTRO-OPTO-MECHANICAL SYSTEM

Our electro-opto-mechanical (EOM) converter consists of a mechanical resonator (MR) that is capacitively coupled on one side to a driven superconducting microwave cavity, and on the other side to a driven Fabry-Pérot optical cavity [1–3]. These cavities' driving fields are at radian frequencies $\omega_{\mathrm{d},j} = \omega_j - \Delta_{0,j}$, where the $\Delta_{0,j}$ are the detunings from their resonant frequencies ω_j, with $j = \mathrm{w}, o$ denoting the microwave and optical cavities, respectively. We include intrinsic losses for these cavities with rates κ_j^{int}, and use κ_j^{in} to denote their input-port coupling rates. The Hamiltonian of the coupled system in terms of annihilation and creation operators has been studied in Ref. [4], and is given by

$$\begin{aligned}\hat{H} = \hbar\omega_M \hat{b}^\dagger\hat{b} + \hbar\sum_{j=\mathrm{w},o}\omega_j\hat{a}_j^\dagger\hat{a}_j + \frac{\hbar g_{\mathrm{w}}}{2}(\hat{b}^\dagger+\hat{b})(\hat{a}_{\mathrm{w}}+\hat{a}_{\mathrm{w}}^\dagger)^2 + \hbar g_o(\hat{b}^\dagger+\hat{b})\hat{a}_o^\dagger\hat{a}_o \\ +\mathrm{i}\hbar E_{\mathrm{w}}(e^{\mathrm{i}\omega_{\mathrm{d,w}}t} - e^{-\mathrm{i}\omega_{\mathrm{d,w}}t})(\hat{a}_{\mathrm{w}}+\hat{a}_{\mathrm{w}}^\dagger) + \mathrm{i}\hbar E_o(\hat{a}_o^\dagger e^{-\mathrm{i}\omega_{\mathrm{d},o}t} - \hat{a}_o e^{\mathrm{i}\omega_{\mathrm{d},o}t}).\end{aligned} \tag{1}$$

Here, $\hat{b}$ is the annihilation operator of the MR whose resonant frequency is ω_M, $\hat{a}_j$ is the annihilation operator for cavity j whose coupling rate to the MR is g_j. The optical-driving strength is $E_o = \sqrt{2P_o\kappa_o^{\mathrm{in}}/\hbar\omega_{\mathrm{d},o}}$, where P_o is the laser power. The microwave cavity is driven by an electric potential with $e(t) = -\mathrm{i}\sqrt{2\hbar\omega_{\mathrm{w}}L}\,E_{\mathrm{w}}(e^{\mathrm{i}\omega_{\mathrm{d,w}}t} - e^{-\mathrm{i}\omega_{\mathrm{d,w}}t})$ where L is the inductance in the microwave electric circuit and E_{w} describes the amplitude of the microwave driving field [4]. In writing Eq. (1) we have ignored any additional degenerate modes that the optical and microwave cavities might have. Ignoring such modes is justified whenever scattering of photons from the driven mode into other cavity modes can be neglected. That condition prevails, for example, with short cavities whose free spectral ranges greatly exceed the MR's resonant frequency, thus ensuring that only one mode from each cavity interacts with the MR, and that adjacent modes are not excited by the driving fields.

In the interaction picture with respect to $\hbar\omega_{\mathrm{d,w}}a_{\mathrm{w}}^\dagger a_{\mathrm{w}} + \hbar\omega_{\mathrm{d},o}a_o^\dagger a_o$, and neglecting terms oscillating at $\pm 2\omega_{\mathrm{d,w}}$, the system Hamiltonian reduces to

$$\hat{H} = \hbar\omega_M\hat{b}^\dagger\hat{b} + \hbar\sum_{j=\mathrm{w},o}\Big[\Delta_{0,j} + g_j(\hat{b}^\dagger+\hat{b})\Big]\hat{a}_j^\dagger\hat{a}_j + \hat{H}_{\mathrm{dri}}, \tag{2}$$

where the Hamiltonian associated with the driving fields is $\hat{H}_{\mathrm{dri}} = \mathrm{i}\hbar\sum_{j=\mathrm{w},o}E_j(\hat{a}_j^\dagger - \hat{a}_j)$.

II. LINEARIZATION OF THE HAMILTONIAN

We can linearize Hamiltonian (2) by expanding the cavity modes around their steady-state field amplitudes, $\hat{c}_j = \hat{a}_j - \sqrt{N_j}$, where $N_j = |E_j|^2/(\kappa_j^2 + \Delta_j^2) \gg 1$ is the mean number of intracavity photons induced by the microwave or optical pumps [4], the $\kappa_j = \kappa_j^{\mathrm{in}} + \kappa_j^{\mathrm{int}}$ are the total cavity decay rates, and the Δ_j are the effective cavity detunings. It is then convenient to move to the interaction picture with respect to the free Hamiltonian, $\hbar\omega_M\hat{b}^\dagger\hat{b} + \hbar\sum_{j=\mathrm{w},o}\omega_j\hat{a}_j^\dagger\hat{a}_j$, where the linearized Hamiltonian becomes

$$\hat{H} = \hbar\sum_{j=\mathrm{w},o}G_j(\hat{b}\mathrm{e}^{-\mathrm{i}\omega_M t} + \hat{b}^\dagger\mathrm{e}^{\mathrm{i}\omega_M t})(\hat{c}_j^\dagger\mathrm{e}^{\mathrm{i}\Delta_j t} + \hat{c}_j\mathrm{e}^{-\mathrm{i}\Delta_j t}), \tag{3}$$

where $G_j = g_j\sqrt{N_j}$. By setting the effective cavity detunings so that $\Delta_{\mathrm{w}} = -\Delta_o = \omega_M$ and neglecting the terms rotating at $\pm 2\omega_M$, the above Hamiltonian reduces to

$$\hat{H} = \hbar G_o(\hat{c}_o\hat{b} + \hat{b}^\dagger\hat{c}_o^\dagger) + \hbar G_{\mathrm{w}}(\hat{c}_{\mathrm{w}}\hat{b}^\dagger + \hat{b}\hat{c}_{\mathrm{w}}^\dagger), \tag{4}$$

as specified in the paper.

III. QUANTUM LANGEVIN EQUATIONS WITH INTERNAL LOSSES

The full quantum treatment of the system can be given in terms of the quantum Langevin equations in which we add to the Heisenberg equations the quantum noise acting on the mechanical resonator ($\hat{b}_{\mathrm{int}}$ with damping rate γ_M),

as well as the cavities' input fluctuations ($\hat{c}_{j,\ \mathrm{in}}$, for $j = \mathrm{w}, o$, with rates κ_j^{in}), plus the intrinsic losses of the cavity modes ($\hat{c}_{j,\ \mathrm{int}}$, for $j = \mathrm{w}, o$, with loss rates κ_j^{int}). These noises have the correlation functions

$$\langle \hat{c}_{j,\ \mathrm{in}}(t)\hat{c}^{\dagger}_{j,\ \mathrm{in}}(t')\rangle = \langle \hat{c}^{\dagger}_{j,\ \mathrm{in}}(t)\hat{c}_{j,\ \mathrm{in}}(t')\rangle + \delta(t-t') = (\bar{n}_j^T + 1)\delta(t-t'), \tag{5a}$$

$$\langle \hat{c}_{j,\ \mathrm{int}}(t)\hat{c}^{\dagger}_{j,\ \mathrm{int}}(t')\rangle = \langle \hat{c}^{\dagger}_{j,\ \mathrm{int}}(t)\hat{c}_{j,\ \mathrm{int}}(t')\rangle + \delta(t-t') = (\bar{n}_j^{\mathrm{int}} + 1)\delta(t-t'), \tag{5b}$$

$$\langle \hat{b}_{\ \mathrm{int}}(t)\hat{b}^{\dagger}{}_{\mathrm{int}}(t')\rangle = \langle \hat{b}^{\dagger}{}_{\mathrm{int}}(t)\hat{b}_{\ \mathrm{int}}(t')\rangle + \delta(t-t') = (\bar{n}_b^T + 1)\delta(t-t'), \tag{5c}$$

where $\bar{n}_j{}^{\mathrm{int}}$, $\bar{n}_j^T$, and $\bar{n}_b^T$ are the Planck-law thermal occupancies of each bath. The resulting Langevin equations for the cavity modes and MR are

$$\dot{\hat{c}}_{\mathrm{w}} = -\kappa_{\mathrm{w}}\hat{c}_{\mathrm{w}} - \mathrm{i}G_{\mathrm{w}}\hat{b} + \sqrt{2\kappa_{\mathrm{w}}^{\mathrm{in}}}\hat{c}_{\mathrm{w,in}} + \sqrt{2\kappa_{\mathrm{w}}^{\mathrm{int}}}\hat{c}_{\mathrm{w,int}}, \tag{6a}$$

$$\dot{\hat{c}}_{o} = -\kappa_{o}\hat{c}_{o} - \mathrm{i}G_{o}\hat{b}^{\dagger} + \sqrt{2\kappa_{o}^{\mathrm{in}}}\hat{c}_{o,\mathrm{in}} + \sqrt{2\kappa_{o}^{\mathrm{int}}}\hat{c}_{o,\mathrm{int}}, \tag{6b}$$

$$\dot{\hat{b}} = -\gamma_M\hat{b} - \mathrm{i}G_{o}\hat{c}_{o}^{\dagger} - \mathrm{i}G_{\mathrm{w}}\hat{c}_{\mathrm{w}} + \sqrt{2\gamma_M}\hat{b}_{\ \mathrm{int}}. \tag{6c}$$

We can solve the above equations in the Fourier domain to obtain the microwave and optical cavities' variables. By substituting the solutions of Eqs. (6a)–(6c) into the corresponding input-output formula for the cavities' variables, i.e., $\hat{d}_j \equiv \hat{c}_{j,\mathrm{out}} = \sqrt{2\kappa_j^{\mathrm{in}}}\hat{c}_j - \hat{c}_{j,\mathrm{in}}$, we obtain

$$\hat{d}_{\mathrm{w}} = A_{\mathrm{w}}(\omega)\hat{c}_{\mathrm{w,in}} - B(\omega)\hat{c}^{\dagger}_{o,\mathrm{in}} - C_{\mathrm{w}}(\omega)\hat{b}_{\mathrm{int}} - D_{\mathrm{w}}(\omega)\hat{c}^{\dagger}_{o,\mathrm{int}} - E_{\mathrm{w}}(\omega)\hat{c}_{\mathrm{w,int}}, \tag{7a}$$

$$\hat{d}_{o} = A_{o}(\omega)\hat{c}_{o,\mathrm{in}} + B^{*}(\omega)\hat{c}^{\dagger}_{\mathrm{w,in}} - C_{o}(\omega)\hat{b}^{\dagger}_{\mathrm{int}} + D_{o}(\omega)\hat{c}^{\dagger}_{\mathrm{w,int}} + E_{o}(\omega)\hat{c}_{o,\mathrm{int}}, \tag{7b}$$

where

$$A_{\mathrm{w}}(\omega) = \frac{[\tilde{\omega}_{\mathrm{w}} - 2\kappa_{\mathrm{w}}^{\mathrm{in}}/\kappa_{\mathrm{w}}][\Gamma_o - \tilde{\omega}_o\tilde{\omega}_b] - \Gamma_{\mathrm{w}}\tilde{\omega}_o}{\tilde{\omega}_{\mathrm{w}}[\tilde{\omega}_o\tilde{\omega}_b - \Gamma_o] + \Gamma_{\mathrm{w}}\tilde{\omega}_o}, \tag{8a}$$

$$A_{o}(\omega) = \frac{-[\tilde{\omega}_o^* - 2\kappa_o^{\mathrm{in}}/\kappa_o][\Gamma_{\mathrm{w}} + \tilde{\omega}_{\mathrm{w}}^*\tilde{\omega}_b^*] + \Gamma_o\tilde{\omega}_{\mathrm{w}}^*}{\tilde{\omega}_{\mathrm{w}}^*[\tilde{\omega}_o^*\tilde{\omega}_b^* - \Gamma_o] + \Gamma_{\mathrm{w}}\tilde{\omega}_o^*}, \tag{8b}$$

$$B(\omega) = 2\sqrt{\frac{\kappa_o^{\mathrm{in}}}{\kappa_o}}\sqrt{\frac{\kappa_{\mathrm{w}}^{\mathrm{in}}}{\kappa_{\mathrm{w}}}}\frac{\sqrt{\Gamma_{\mathrm{w}}\Gamma_o}}{\tilde{\omega}_{\mathrm{w}}[\tilde{\omega}_o\tilde{\omega}_b - \Gamma_o] + \Gamma_{\mathrm{w}}\tilde{\omega}_o}, \tag{8c}$$

$$C_{\mathrm{w}}(\omega) = \sqrt{\frac{\kappa_{\mathrm{w}}^{\mathrm{in}}}{\kappa_{\mathrm{w}}}}\frac{2\mathrm{i}\sqrt{\Gamma_{\mathrm{w}}}\tilde{\omega}_o}{\tilde{\omega}_{\mathrm{w}}[\tilde{\omega}_o\tilde{\omega}_b - \Gamma_o] + \Gamma_{\mathrm{w}}\tilde{\omega}_o}, \tag{8d}$$

$$C_{o}(\omega) = \sqrt{\frac{\kappa_o^{\mathrm{in}}}{\kappa_o}}\frac{2\mathrm{i}\sqrt{\Gamma_o}\tilde{\omega}_{\mathrm{w}}^*}{\tilde{\omega}_{\mathrm{w}}^*[\tilde{\omega}_o^*\tilde{\omega}_b^* - \Gamma_o] + \Gamma_{\mathrm{w}}\tilde{\omega}_o^*}, \tag{8e}$$

$$D_{\mathrm{w}}(\omega) = 2\sqrt{\frac{\kappa_o^{\mathrm{int}}}{\kappa_o}}\sqrt{\frac{\kappa_{\mathrm{w}}^{\mathrm{in}}}{\kappa_{\mathrm{w}}}}\frac{\sqrt{\Gamma_o\Gamma_{\mathrm{w}}}}{\tilde{\omega}_{\mathrm{w}}[\tilde{\omega}_o\tilde{\omega}_b - \Gamma_o] + \Gamma_{\mathrm{w}}\tilde{\omega}_o}, \tag{8f}$$

$$D_{o}(\omega) = 2\sqrt{\frac{\kappa_o^{\mathrm{in}}}{\kappa_o}}\sqrt{\frac{\kappa_{\mathrm{w}}^{\mathrm{int}}}{\kappa_{\mathrm{w}}}}\frac{\sqrt{\Gamma_o\Gamma_{\mathrm{w}}}}{\tilde{\omega}_{\mathrm{w}}^*[\tilde{\omega}_o^*\tilde{\omega}_b^* - \Gamma_o] + \Gamma_{\mathrm{w}}\tilde{\omega}_o^*}, \tag{8g}$$

$$E_{\mathrm{w}}(\omega) = 2\sqrt{\frac{\kappa_{\mathrm{w}}^{\mathrm{int}}}{\kappa_{\mathrm{w}}}}\sqrt{\frac{\kappa_{\mathrm{w}}^{\mathrm{in}}}{\kappa_{\mathrm{w}}}}\frac{\Gamma_o - \tilde{\omega}_o\tilde{\omega}_b}{\tilde{\omega}_{\mathrm{w}}[\tilde{\omega}_o\tilde{\omega}_b - \Gamma_o] + \Gamma_{\mathrm{w}}\tilde{\omega}_o}, \tag{8h}$$

$$E_{o}(\omega) = 2\sqrt{\frac{\kappa_o^{\mathrm{int}}}{\kappa_o}}\sqrt{\frac{\kappa_o^{\mathrm{in}}}{\kappa_o}}\frac{\Gamma_{\mathrm{w}} + \tilde{\omega}_{\mathrm{w}}^*\tilde{\omega}_b^*}{\tilde{\omega}_{\mathrm{w}}^*[\tilde{\omega}_o^*\tilde{\omega}_b^* - \Gamma_o] + \Gamma_{\mathrm{w}}\tilde{\omega}_o^*}, \tag{8i}$$

with $\tilde{\omega}_j = 1 - \mathrm{i}\omega/\kappa_j$, $\tilde{\omega}_b = 1 - \mathrm{i}\omega/\gamma_M$, and $\Gamma_j = G_j^2/\kappa_j\gamma_M$. The coefficients (8a)–(8i) become much simpler at $\omega \simeq 0$, which corresponds to take a narrow frequency band around each cavity resonance, viz.,

$$A_\mathrm{w} = \frac{[1-2\kappa_\mathrm{w}^\mathrm{in}/\kappa_\mathrm{w}][\Gamma_o - 1] - \Gamma_\mathrm{w}}{1-\Gamma_o+\Gamma_\mathrm{w}}, \tag{9a}$$

$$A_o = \frac{-[1-2\kappa_o^\mathrm{in}/\kappa_o][\Gamma_\mathrm{w} + 1] + \Gamma_o}{1-\Gamma_o+\Gamma_\mathrm{w}}, \tag{9b}$$

$$B = 2\sqrt{\frac{\kappa_o^\mathrm{in}}{\kappa_o}}\sqrt{\frac{\kappa_\mathrm{w}^\mathrm{in}}{\kappa_\mathrm{w}}}\frac{\sqrt{\Gamma_\mathrm{w}\Gamma_o}}{1-\Gamma_o+\Gamma_\mathrm{w}}, \tag{9c}$$

$$C_\mathrm{w} = \sqrt{\frac{\kappa_\mathrm{w}^\mathrm{in}}{\kappa_\mathrm{w}}}\frac{2\mathrm{i}\sqrt{\Gamma_\mathrm{w}}}{1-\Gamma_o+\Gamma_\mathrm{w}}, \tag{9d}$$

$$C_o = \sqrt{\frac{\kappa_o^\mathrm{in}}{\kappa_o}}\frac{2\mathrm{i}\sqrt{\Gamma_o}}{1-\Gamma_o+\Gamma_\mathrm{w}}, \tag{9e}$$

$$D_\mathrm{w} = 2\sqrt{\frac{\kappa_o^\mathrm{int}}{\kappa_o}}\sqrt{\frac{\kappa_\mathrm{w}^\mathrm{in}}{\kappa_\mathrm{w}}}\frac{\sqrt{\Gamma_o\Gamma_\mathrm{w}}}{1-\Gamma_o+\Gamma_\mathrm{w}}, \tag{9f}$$

$$D_o = 2\sqrt{\frac{\kappa_o^\mathrm{in}}{\kappa_o}}\sqrt{\frac{\kappa_\mathrm{w}^\mathrm{int}}{\kappa_\mathrm{w}}}\frac{\sqrt{\Gamma_o\Gamma_\mathrm{w}}}{1-\Gamma_o+\Gamma_\mathrm{w}}, \tag{9g}$$

$$E_\mathrm{w} = 2\sqrt{\frac{\kappa_\mathrm{w}^\mathrm{int}}{\kappa_\mathrm{w}}}\sqrt{\frac{\kappa_\mathrm{w}^\mathrm{in}}{\kappa_\mathrm{w}}}\frac{\Gamma_o - 1}{1-\Gamma_o+\Gamma_\mathrm{w}}, \tag{9h}$$

$$E_o = 2\sqrt{\frac{\kappa_o^\mathrm{int}}{\kappa_o}}\sqrt{\frac{\kappa_o^\mathrm{in}}{\kappa_o}}\frac{\Gamma_\mathrm{w} + 1}{1-\Gamma_o+\Gamma_\mathrm{w}}. \tag{9i}$$

Furthermore, when the internal losses are negligible, i.e., $\kappa_j^\mathrm{int}/\kappa_j^\mathrm{in} \ll 1$, then we get $D_j = E_j \simeq 0$, and Eqs. (7a)–(7b) reduce to the simple forms presented in the paper,

$$\hat{d}_\mathrm{w} = A_\mathrm{w}\hat{c}_\mathrm{w,in} - B\hat{c}_{o,\mathrm{in}}^\dagger - C_\mathrm{w}\hat{b}_\mathrm{int}, \tag{10a}$$

$$\hat{d}_\mathrm{o} = B\hat{c}_\mathrm{w,in,}^\dagger + A_\mathrm{o}\hat{c}_{o,\mathrm{in}} - C_\mathrm{o}\hat{b}_\mathrm{int}^\dagger, \tag{10b}$$

with coefficients given by

$$A_\mathrm{w} = \frac{1-(\Gamma_\mathrm{w}+\Gamma_o)}{1+\Gamma_\mathrm{w}-\Gamma_o}, \tag{11a}$$

$$A_o = \frac{1+(\Gamma_\mathrm{w}+\Gamma_o)}{1+\Gamma_\mathrm{w}-\Gamma_o}, \tag{11b}$$

$$B = \frac{2\sqrt{\Gamma_\mathrm{w}\Gamma_o}}{1+\Gamma_\mathrm{w}-\Gamma_o}, \tag{11c}$$

$$C_o = \frac{2\mathrm{i}\sqrt{\Gamma_o}}{1+\Gamma_\mathrm{w}-\Gamma_o}, \tag{11d}$$

$$C_\mathrm{w} = \frac{2\mathrm{i}\sqrt{\Gamma_\mathrm{w}}}{1+\Gamma_\mathrm{w}-\Gamma_o}. \tag{11e}$$

These input-output relations preserve the bosonic commutation relations, i.e., when the operators on the right in Eqs. (10a) and (10b) satisfy those commutation relations, we get $[\hat{d}_i, \hat{d}_j^\dagger] = \delta_{i,j}$ and $[\hat{d}_i, \hat{d}_j] = [\hat{d}_i^\dagger, \hat{d}_j^\dagger] = 0$, for $i, j \in \mathrm{w}, o$.

IV. MICROWAVE-OPTICAL ENTANGLEMENT

A. Entanglement Metric

Equations (10a) and (10b) are driven by a collection of independent, thermal-state inputs, $\hat{c}_{\mathrm{w,in}}$, $\hat{c}_{o,\mathrm{in}}$, and $\hat{b}_{\mathrm{int}}$ and their adjoints. Consequently, those equations' outputs, $\hat{d}_{\mathrm{w}}$ and $\hat{d}_o$, are in a zero-mean, jointly-Gaussian state that is completely characterized by its non-zero second moments,

$$\bar{n}_{\mathrm{w}} \equiv \langle \hat{d}_{\mathrm{w}}^{\dagger} \hat{d}_{\mathrm{w}} \rangle = |A_{\mathrm{w}}|^2 \bar{n}_{\mathrm{w}}^T + |B|^2 (\bar{n}_o^T + 1) + |C_{\mathrm{w}}|^2 \bar{n}_b^T, \tag{12a}$$

$$\bar{n}_o \equiv \langle \hat{d}_o^{\dagger} \hat{d}_o \rangle = |B|^2 (\bar{n}_{\mathrm{w}}^T + 1) + |A_o|^2 \bar{n}_o^T + |C_o|^2 (\bar{n}_b^T + 1), \tag{12b}$$

$$\langle \hat{d}_{\mathrm{w}} \hat{d}_o \rangle = A_{\mathrm{w}} B (\bar{n}_{\mathrm{w}}^T + 1) - B A_o \bar{n}_o^T + C_{\mathrm{w}} C_o (\bar{n}_b^T + 1). \tag{12c}$$

That joint state will be *classical*, i.e., have a proper P-representation, if and only if the phase-sensitive cross correlation, $|\langle \hat{d}_{\mathrm{w}} \hat{d}_o \rangle|$, satisfies the classical bound [5]

$$|\langle \hat{d}_{\mathrm{w}} \hat{d}_o \rangle| \leq \sqrt{\bar{n}_{\mathrm{w}} \bar{n}_o}. \tag{13}$$

When $|\langle \hat{d}_{\mathrm{w}} \hat{d}_o \rangle|$ violates this bound, the microwave (w) and optical (o) modes are entangled. Note that, regardless of whether the *classical* bound is violated, the absence of phase-sensitive second moments in the joint state, viz., $\langle \hat{d}_{\mathrm{w}}^2 \rangle = \langle \hat{d}_o^2 \rangle = 0$, implies that the reduced density operators for these individual modes are thermal states. The average photon numbers for the microwave and optical modes also put a *quantum* upper limit on $|\langle \hat{d}_{\mathrm{w}} \hat{d}_o \rangle|$, given by [6]

$$|\langle \hat{d}_{\mathrm{w}} \hat{d}_o \rangle| \leq \sqrt{\max(\bar{n}_{\mathrm{w}}, \bar{n}_o)[1 + \min(\bar{n}_{\mathrm{w}}, \bar{n}_o)]}, \tag{14}$$

which can be saturated when $\bar{n}_{\mathrm{w}} = \bar{n}_o$, but not when $\bar{n}_{\mathrm{w}} \neq \bar{n}_o$.

Figure 2 in the main paper plots—versus Γ_{w} and Γ_o, and assuming experimentally-accessible parameter values—the entanglement metric

$$\mathcal{E} \equiv \frac{|\langle \hat{d}_{\mathrm{w}} \hat{d}_o \rangle|}{\sqrt{\bar{n}_{\mathrm{w}} \bar{n}_o}}, \tag{15}$$

which exceeds unity if and only if the microwave and optical modes are entangled. The entanglement metric provides a very simple entanglement criterion and, as we can see from the figure in the main paper, our microwave-optical source is proven to have wide regions of parameters where $\mathcal{E} > 1$.

B. Logarithmic Negativity and Coherent Information

Here we quantify the amount of entanglement generated by our microwave-optical source using standard measures in quantum information theory. In particular, we consider the log-negativity [7] and the coherent information [8], which are, respectively, an upper and a lower bound to the number of distillable entanglement bits (ebits) generated by the source. We normalize these measures by the mean number of microwave signal photons $\bar{n}_{\mathrm{w}}$ sent to the target. The rationale behind this normalization is physical and strictly connected with the specific model considered.

In fact, quantum illumination (QI) is a energy-constrained protocol, where quantum and classical sources are compared by fixing the mean number of photons in the signal mode [9], which corresponds to the microwave mode in the present case. Thus, it is intuitively expected that, at fixed $\bar{n}_{\mathrm{w}}$, the advantage of quantum illumination increases by increasing the amount of quantum entanglement (and more generally, quantum correlations) present in the source.

For this reason, the quality of the source can be estimated in two ways: (1) At fixed $\bar{n}_{\mathrm{w}}$, we optimize the entanglement of the quantum source, or (2) we maximize the entanglement of the quantum source normalized by $\bar{n}_{\mathrm{w}}$, i.e., the average entanglement carried by each microwave photon. The two options are clearly connected since, at fixed $\bar{n}_{\mathrm{w}}$, the most entangled source is the one emitting more ebits per microwave photon. However, the second option is more flexible to use, since it can be applied to the cases where $\bar{n}_{\mathrm{w}}$ changes in terms of the various parameters of the problem, as it happens here on the cooperativity plane (Γ_o,Γ_{w}).

1. Logarithmic Negativity

In order to compute the log-negativity, we first determine the covariance matrix (CM) of our system in the frequency domain, which can be expressed as

$$\delta(\omega+\omega')V_{ij}(\omega)=\frac{1}{2}\langle u_i(\omega)u_j(\omega')+u_j(\omega')u_i(\omega)\rangle, \tag{16}$$

where

$$\mathbf{u}(\omega)=[X_{\rm w}(\omega),Y_{\rm w}(\omega),X_o(\omega),Y_o(\omega)]^T, \tag{17}$$

and $X_j=(d_j+d_j^\dagger)/\sqrt{2}$, $Y_j=(d_j-d_j^\dagger)/\mathrm{i}\sqrt{2}$ with $j=o,\mathrm{w}$. Note that the vacuum noise has variance $1/2$ in these quadratures.

Now, by using Eqs. (10a), (10b) and (16), we obtain the CM for the quadratures of the microwave and optical cavities' outputs, which is given by the normal form

$$\mathbf{V}(\omega)=\begin{pmatrix} V_{11} & 0 & V_{13} & 0\\ 0 & V_{11} & 0 & -V_{13}\\ V_{13} & 0 & V_{33} & 0\\ 0 & -V_{13} & 0 & V_{33}\end{pmatrix}, \tag{18}$$

where we explicitly have

$$V_{11}=\frac{\langle X_{\rm w}(\omega)X_{\rm w}(\omega')\rangle}{\delta(\omega+\omega')}=\bar{n}_{\rm w}+1/2, \tag{19a}$$

$$V_{33}=\frac{\langle X_o(\omega)X_o(\omega')\rangle}{\delta(\omega+\omega')}=\bar{n}_o+1/2, \tag{19b}$$

$$V_{13}=\frac{\langle X_{\rm w}(\omega)X_o(\omega')+X_o(\omega')X_{\rm w}(\omega)\rangle}{2\delta(\omega+\omega')}=\langle\hat{d}_{\rm w}\hat{d}_o\rangle, \tag{19c}$$

and we have used the fact that $\langle\hat{d}_{\rm w}\hat{d}_o\rangle$ is real valued. Note that Eq. (18) is the typical CM of a two-mode squeezed thermal state [10].

The log-negativity E_N is given by [7]

$$E_N=\max[0,-\log(2\zeta^-)], \tag{20}$$

where ζ^- is the smallest partially-transposed symplectic eigenvalue of $\mathbf{V}(\omega)$, given by [11]

$$\zeta^-=2^{-1/2}\left(V_{11}^2+V_{33}^2+2V_{13}^2-\sqrt{(V_{11}^2-V_{33}^2)^2+4V_{13}^2(V_{11}+V_{33})^2}\right)^{1/2}. \tag{21}$$

In Fig. 2 of the main paper, we have plotted the normalized log-negativity $E_N/\bar{n}_{\rm w}$ versus the cooperativities, $\Gamma_{\rm w}$ and Γ_o. From panel (b) of that figure, we can see the presence of a wide region where the quality of the source is very good in terms of ebits of log-negativity per microwave photon emitted.

It is easy to show that $E_N=0$ for $\mathcal{E}\leq 1$. Moreover, for the case of interest for QI—in which $\bar{n}_j\equiv\langle\hat{d}_j^\dagger\hat{d}_j\rangle\leq 1$ for $j=\mathrm{w},o$—we find that $2\zeta^-$ decreases monotonically, at fixed $\bar{n}_{\rm w}$ and $\bar{n}_o$, as $|\langle\hat{d}_{\rm w}\hat{d}_o\rangle|$ increases from zero to its quantum upper bound from Eq. (14). Thus, given $\bar{n}_j\leq 1$ for $j=\mathrm{w},o$, the logarithmic negativity E_N for our source can be related with the entanglement metric $\mathcal{E}$.

2. Coherent Information

Here we compute the coherent information associated with our microwave-optical source. This is given by [8]

$$I(o\rangle\mathrm{w})=S(\mathrm{w})-S(o,\mathrm{w}), \tag{22}$$

where $S(\mathrm{w})$ is the von Neumann entropy [11] of the microwave mode, while $S(o,\mathrm{w})$ is the joint von Neumann entropy of the optical and microwave modes. As mentioned before, this provides a lower bound to the number of ebits which

are distillable from the source. In fact, according to the hashing inequality [12], $I(o\rangle\mathrm{w})$ gives the distillation rate (ebits per use of the source) which is achievable by distillation protocols based on one-way classical communication (here directed from the optical to the microwave part).

For a Gaussian state, like our source, we can simply express the entropic terms in Eq. (22) in terms of the symplectic eigenvalue ν_{w} of the reduced CM associated with the microwave mode and the symplectic spectrum $\{\nu_-,\nu_+\}$ of the global CM $\mathbf{V}(\omega)$ associated with the microwave and optical modes. These eigenvalues are given by $\nu_{\mathrm{w}}=V_{11}$ and [11]

$$\nu_{\pm}=2^{-1/2}\left(V_{11}^2+V_{33}^2-2V_{13}^2\pm\sqrt{(V_{11}^2-V_{33}^2)^2-4V_{13}^2(V_{11}-V_{33})^2}\right)^{1/2}. \tag{23}$$

Thus, we have [11]

$$I(o\rangle\mathrm{w})=h(V_{11})-h(\nu_-)-h(\nu_+), \tag{24}$$

where [13]

$$h(x)\equiv\left(x+\frac{1}{2}\right)\log_2\left(x+\frac{1}{2}\right)-\left(x-\frac{1}{2}\right)\log_2\left(x-\frac{1}{2}\right). \tag{25}$$

In Fig. 2 of the main paper, we have plotted the normalized coherent information $I(o\rangle\mathrm{w})/\bar{n}_{\mathrm{w}}$ versus the cooperativities, Γ_{w} and Γ_o. From panel (c) of that figure, we can see the presence of a wide region where the quality of the source is good in terms of qubits of coherent information per microwave photon emitted (lower bound to the number of ebits per microwave photon). Finally, note that the computation of the normalized *reverse* coherent information [14, 15] $I(o\langle\mathrm{w})/\bar{n}_{\mathrm{w}}$ (where the direction of the classical communication is inverted from the microwave to the optical part) leads to completely similar results, as shown in Fig. 1.

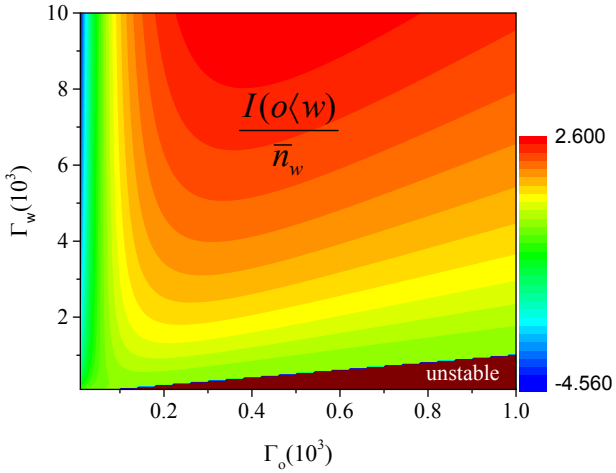

FIG. 1. Normalized reverse coherent information $I(o\langle\mathrm{w})/\bar{n}_{\mathrm{w}}$ (qubits per microwave photon) plotted on the cooperativity plane $(\Gamma_o,\Gamma_{\mathrm{w}})$. See Fig. 2 of the main paper for the other parameter values.

V. MICROWAVE-OPTICAL QUANTUM CORRELATIONS BEYOND ENTANGLEMENT

Our microwave-optical source generates a Gaussian state which is mixed, as one can easily check from the numerical values of its von Neumann entropy $S(o,\mathrm{w})$. It is therefore important to describe its quality also in terms of general quantum correlations beyond quantum entanglement. Thus we compute here the quantum discord [16] of the source $D(\mathrm{w}|o)$, capturing the basic quantum correlations which are carried by the microwave mode sent to target. Such quantity is normalized by $\bar{n}_{\mathrm{w}}$, for the same reasons we have previously explained for quantum entanglement: The best sources for our QI problem are expected to be those maximizing the amount of quantum correlations per microwave photon emitted.

Since our source emits a mixed Gaussian state which is a two-mode squeezed thermal state, we can compute its (unrestricted) quantum discord using the formulas of Ref. [10]. In particular, the CM in Eq. (18) can be expressed as [10]

$$\mathbf{V}(\omega) = \begin{pmatrix} (\tau b + \eta)\mathbf{I} & \sqrt{\tau(b^2-1)}\mathbf{Z} \\ \sqrt{\tau(b^2-1)}\mathbf{Z} & b\mathbf{I} \end{pmatrix}, \quad \begin{matrix} \mathbf{I} \equiv \mathrm{diag}(1,1), \\ \mathbf{Z} \equiv \mathrm{diag}(1,-1), \end{matrix} \tag{26}$$

where

$$b = V_{33}, \quad \tau = \frac{V_{13}^2}{V_{33}^2 - 1}, \quad \eta = V_{11} - \frac{V_{33}V_{13}^2}{V_{33}^2 - 1}. \tag{27}$$

Thus, we may write [10]

$$D(\mathrm{w}|o) = h(b) - h(\nu_-) - h(\nu_+) + h(\tau + \eta) \tag{28}$$

$$= h(V_{33}) - h(\nu_-) - h(\nu_+) + h\left[V_{11} + \frac{V_{13}^2(1 - V_{33})}{V_{33}^2 - 1}\right], \tag{29}$$

where ν_- and ν_+ are the symplectic eigenvalues of $\mathbf{V}(\omega)$.

In Fig. 2 of the main paper, we have plotted the normalized quantum discord $D(\mathrm{w}|o)/\bar{n}_\mathrm{w}$ versus the cooperativities, Γ_w and Γ_o. From panel (d) of that figure, we can see the presence of a wide region where the quality of the source is very good in terms of discordant bits per microwave photon emitted. Furthermore, the similarity between this normalized measure and the final QI avantage (figure 4 of the main paper) is remarkable.

Finally, note that the computation of the normalized version of the other quantum discord [16] $D(o|\mathrm{w})/\bar{n}_\mathrm{w}$ leads to similar results, as shown below in Fig. 2 of this Supplemental Material.

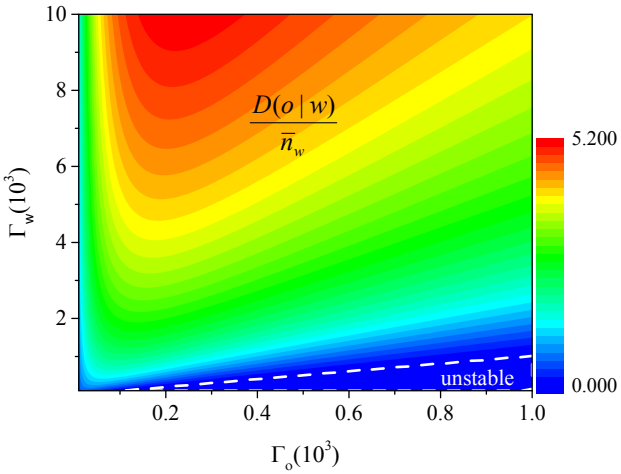

FIG. 2. Normalized quantum discord $D(o|\mathrm{w})/\bar{n}_\mathrm{w}$ (discordant bits per microwave photon) plotted on the cooperativity plane $(\Gamma_o, \Gamma_\mathrm{w})$. See Fig. 2 of the main paper for the other parameter values.

VI. ERROR PROBABILITY FOR M MODE PAIRS

Our transmitter's EOM converter is governed by Eqs. (10a) and (10b) in which the coefficients appearing therein are as specified in Eqs. (11a)–(11e). These same coefficients appear in the input-output relation

$$\hat{d}_{\eta,\mathrm{o}} = B\hat{c}_R^\dagger + A_\mathrm{o}\hat{c}'_{\mathrm{o,in}} - C_\mathrm{o}\hat{b}'^\dagger_{\mathrm{int}}, \tag{30}$$

for the QI receiver's EOM converter. Equations (10a) and (10b) apply to one of the $M = t_m W_m \gg 1$ independent, identically-distributed (iid) mode pairs produced by the bandwidth-W_m, continuous-wave transmitter during the t_m-sec-duration measurement interval used to discriminate target absence from target presence. Under either hypothesis

(target absent or present), the QI receiver takes as its inputs M iid mode pairs, $\{\hat{c}_R^{(k)}, \hat{d}_o^{(k)} : 1 \le k \le M\}$ that are in a zero-mean, jointly-Gaussian state characterized by the conditional (given target absence or presence) second moments: $\langle \hat{c}_R^{(k)\dagger} \hat{c}_R^{(k)} \rangle_{H_j}$, $\langle \hat{d}_o^{(k)\dagger} \hat{d}_o^{(k)} \rangle$, and $\langle \hat{c}_R^{(k)} \hat{d}_o^{(k)} \rangle_{H_j}$. The receiver's EOM converter transforms the returned microwave modes, $\hat{c}_R^{(k)}$, into optical modes, $\hat{d}_{\eta,o}^{(k)}$, such that the $\{\hat{d}_{\eta,o}^{(k)}, \hat{d}_o^{(k)} : 1 \le k \le M\}$ are iid mode pairs which, under either hypothesis, are in a zero-mean jointly-Gaussian state characterized by the second moments $\langle \hat{d}_{\eta,o}^{(k)\dagger} \hat{d}_{\eta,o}^{(k)} \rangle_{H_j}$, $\langle \hat{d}_o^{(k)\dagger} \hat{d}_o^{(k)} \rangle$, and $\langle \hat{d}_{\eta,o}^{(k)} \hat{d}_o^{(k)} \rangle_{H_j}$. Note that, in addition to its transforming the microwave modes into optical modes, the EOM converter transforms the *phase-sensitive* cross correlations, $\{\langle \hat{c}_R^{(k)} \hat{d}_o^{(k)} \rangle_{H_1}\}$, into *phase-insensitive* cross correlations, $\{\langle \hat{d}_{\eta,o}^{(k)} \hat{d}_o^{(k)} \rangle_{H_1}\}$, which can be measured—as shown in Fig. 3—by mixing returned and retained modes on a 50–50 beam splitter whose outputs are

$$\hat{a}_{\eta,\pm}^{(k)} \equiv \frac{\hat{d}_{\eta,o}^{(k)} \pm \hat{d}_o^{(k)}}{\sqrt{2}}. \tag{31}$$

These modes are then photodetected, yielding modal photon-counts that are equivalent to measurements of the number operators $\hat{N}_{\eta,\pm}^{(k)} \equiv \hat{a}_{\eta,\pm}^{(k)\dagger} \hat{a}_{\eta,\pm}^{(k)}$. Finally, the target absence-or-presence decision is made by comparing the difference of the two detectors' total photon counts [17], which is equivalent to the quantum measurement

$$\hat{N}_\eta = \sum_{k=1}^{M} \left(\hat{N}_{\eta,+}^{(k)} - \hat{N}_{\eta,-}^{(k)} \right), \tag{32}$$

with a threshold chosen to make the receiver's false-alarm probability

$$P_F \equiv \Pr(\text{decide target present} \mid \text{target absent}), \tag{33}$$

equals its miss probability,

$$P_M \equiv \Pr(\text{decide target absent} \mid \text{target present}). \tag{34}$$

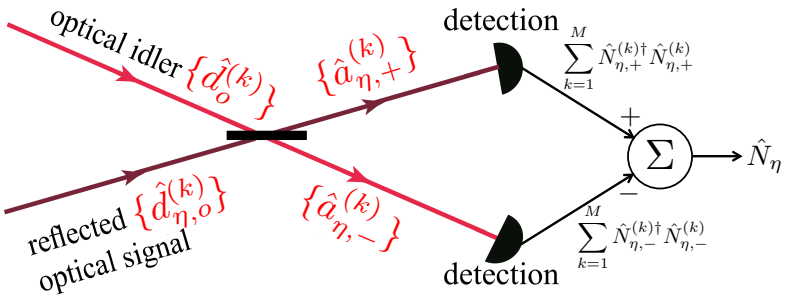

FIG. 3. Optical post-processing in the QI receiver. A 50-50 beam splitter mixes the wavelength-converted return modes $\{\hat{d}_{\eta,o}^{(k)}\}$, from the receiver's EOM converter with the retained idler modes, $\{\hat{d}_o^{(k)}\}$. The beam splitter's outputs are detected, yielding classical outcomes equivalent to the quantum measurements $\sum_{k=1}^{M} \hat{N}_{\eta,\pm}^{(k)}$, and the difference of these outputs, equivalent to the quantum measurement of $\hat{N}_\eta$, is used as the input to a threshold detector (not shown) whose output is the target absence or presence decision.

Because QI employs an enormous number of mode pairs, and those mode pairs are iid under both hypotheses, the Central Limit Theorem implies that the $\hat{N}_\eta$ measurement yields a random variable that is Gaussian, conditioned on target absence or target presence. It follows that the QI receiver's error probability, for equally-likely hypotheses, satisfies

$$P_{\text{QI}}^{(M)} = \frac{P_F + P_M}{2} = \frac{\text{erfc}\left(\sqrt{\text{SNR}_{\text{QI}}^{(M)}/8} \right)}{2}, \tag{35}$$

where the M-mode signal-to-noise ratio is

$$\text{SNR}_{\text{QI}}^{(M)} = \frac{4(\langle \hat{N}_\eta \rangle_{H_1} - \langle \hat{N}_\eta \rangle_{H_0})^2}{\left(\sqrt{\langle \Delta \hat{N}_\eta^2 \rangle_{H_0}} + \sqrt{\langle \Delta \hat{N}_\eta^2 \rangle_{H_1}} \right)^2}, \tag{36}$$

with $\langle \hat{N}_\eta \rangle_{H_j}$ and $\langle \Delta \hat{N}_\eta^2 \rangle_{H_j}$, for $j = 0, 1$, being the conditional means and conditional variances of $\hat{N}_\eta$.

The iid nature of the $\{\hat{N}_{\eta,+}^{(k)}, \hat{N}_{\eta,-}^{(k)}\}$ allow us to rewrite the M-mode SNR in terms of single-mode moments, i.e.,

$$\mathrm{SNR}_{\mathrm{QI}}^{(M)} = \frac{4M[(\langle \hat{N}_{\eta,+} \rangle_{H_1} - \langle \hat{N}_{\eta,-} \rangle_{H_1}) - (\langle \hat{N}_{\eta,+} \rangle_{H_0} - \langle \hat{N}_{\eta,-} \rangle_{H_0})]^2}{\left(\sqrt{\langle (\Delta \hat{N}_{\eta,+} - \Delta \hat{N}_{\eta,-})^2 \rangle_{H_0}} + \sqrt{\langle (\Delta \hat{N}_{\eta,+} - \Delta \hat{N}_{\eta,-})^2 \rangle_{H_1}} \right)^2}, \tag{37}$$

where we have suppressed the superscript $^{(k)}$. The moments needed to instantiate Eq. (37) are now easily found. In particular, for the mean values we find that

$$\langle \hat{N}_{\eta,\pm} \rangle_{H_0} = |B|^2[(\bar{n}_B + \bar{n}_{\mathrm{w}}^T)/2 + 1] + |A_o|^2 \bar{n}_o^T + |C_o|^2(\bar{n}_b^T + 1), \tag{38a}$$

$$\begin{aligned} \langle \hat{N}_{\eta,\pm} \rangle_{H_1} = {} & \langle \hat{N}_{\eta,\pm} \rangle_{H_0} + \eta |B|^2[|A_{\mathrm{w}}|^2(\bar{n}_{\mathrm{w}}^T + 1) + |B|^2 \bar{n}_o^T + |C_{\mathrm{w}}|^2(\bar{n}_b^T + 1)]/2 \\ & \pm \sqrt{\eta}\, \mathrm{Re}[|B|^2 A_{\mathrm{w}}(\bar{n}_{\mathrm{w}}^T + 1) - |B|^2 A_o \bar{n}_o^T + B^* C_{\mathrm{w}} C_o(\bar{n}_b^T + 1)] \end{aligned} \tag{38b}$$

whence

$$\langle \hat{N}_{\eta,+} \rangle_{H_0} - \langle \hat{N}_{\eta,-} \rangle_{H_0} = 0, \tag{39a}$$

$$\langle \hat{N}_{\eta,+} \rangle_{H_1} - \langle \hat{N}_{\eta,-} \rangle_{H_1} = 2\sqrt{\eta}\, \mathrm{Re}[|B|^2 A_{\mathrm{w}}(\bar{n}_{\mathrm{w}}^T + 1) - |B|^2 A_o \bar{n}_o^T + B^* C_{\mathrm{w}} C_o(\bar{n}_b^T + 1)], \tag{39b}$$

For the variances we get [18]

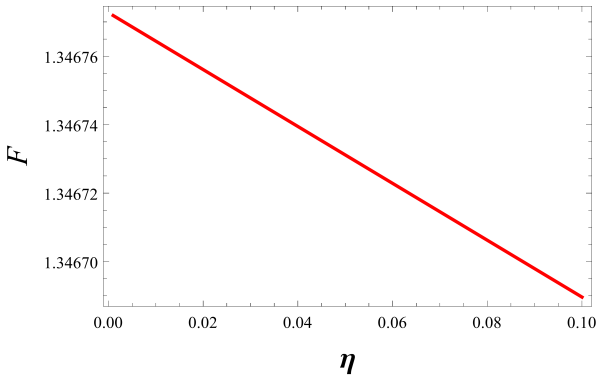

FIG. 4. The dependence of the QI-advantage figure of merit $\mathcal{F} \equiv \mathrm{SNR}_{\mathrm{QI}}^{(M)}/\mathrm{SNR}_{\mathrm{coh}}^{(M)}$ on η. See Fig. 2 of the main paper for the other parameter values.

$$\langle (\Delta \hat{N}_{\eta,+} - \Delta \hat{N}_{\eta,-})^2 \rangle_{H_j} = \langle \hat{N}_{\eta,+} \rangle_{H_j} (\langle \hat{N}_{\eta,+} \rangle_{H_j} + 1) + \langle \hat{N}_{\eta,-} \rangle_{H_j} (\langle \hat{N}_{\eta,-} \rangle_{H_j} + 1) - (\langle \hat{d}_{\eta,o}^\dagger \hat{d}_{\eta,o} \rangle_{H_j} - \langle \hat{d}_o^\dagger \hat{d}_o \rangle)^2/2, \tag{40}$$

for $j = 0, 1$, where

$$\langle \hat{d}_{\eta,o}^\dagger \hat{d}_{\eta,o} \rangle_{H_j} = \begin{cases} |B|^2(\bar{n}_B + 1) + |A_o|^2 \bar{n}_o^T + |C_o|^2(\bar{n}_b^T + 1), & \text{for } j = 0 \\ \langle \hat{d}_{\eta,o}^\dagger \hat{d}_{\eta,o} \rangle_{H_0} + \eta |B|^2[|A_{\mathrm{w}}|^2(\bar{n}_{\mathrm{w}}^T + 1) + |B|^2 \bar{n}_o^T + |C_{\mathrm{w}}|^2(\bar{n}_b^T + 1)], & \text{for } j = 1. \end{cases} \tag{41}$$

It is interesting to see how the transmitter-to-target-to-receiver transmissivity, η, affects QI's performance advantage over coherent-state operation. Figure 4 shows the dependence of the QI-advantage figure of merit $\mathcal{F} \equiv \mathrm{SNR}_{\mathrm{QI}}^{(M)}/\mathrm{SNR}_{\mathrm{coh}}^{(M)}$ for $10^{-3} \leq \eta \leq 10^{-1}$. We have restricted our attention here to the low-η regime, because we follow the lead of [9] in assuming that the target's presence has no passive signature. A passive signature—a lower received background level in the presence of the target—would permit the target to be detected without transmitting any microwave radiation. We preclude that possibility by assuming that the noise mode $\hat{c}_B$ has average photon number $\bar{n}_B$ when the target is absent and average photon number $\bar{n}_B/(1-\eta)$ when the target is present. Unless $\eta \ll 1$, so that these two average photon numbers are nearly the same, this assumption is physically unreasonable.

[1] R. W. Andrews, R. W. Peterson, T. P. Purdy, K. Cicak, R. W. Simmonds, C. A. Regal, and K. W. Lehnert, Nature Phys. **10,** 321 (2014).

[2] J. Bochmann, A. Vainsencher, D. D. Awschalom, and A. N. Cleland, Nature Phys. **9,** 712 (2013).

[3] T. Bagci, A. Simonsen, S. Schmid, L. G. Villanueva, E. Zeuthen, J. Appel, J. M. Taylor, A. Sørensen, A. Schliesser, and E. S. Polzik, Nature **507,** 81 (2014).

[4] Sh. Barzanjeh, D. Vitali, P. Tombesi, and G. J. Milburn, Phys. Rev. A **84,** 042342 (2011).

[5] The classical bound arises from the requirement that $\langle |x d_{\rm w} + d_o^*|^2 \rangle \geq 0$ for classical, complex-valued random variables $d_{\rm w}$ and d_o, where $\langle \cdot \rangle$ denotes classical ensemble average and x is an arbitrary real-valued parameter.

[6] The quantum bound arises from the requirement that $\langle (x\hat{d}_{\rm w} \ + \hat{d}_o^\dagger)^\dagger (x\hat{d}_{\rm w} \ + \hat{d}_o^\dagger) \rangle \geq 0$ *and* $\langle (x\hat{d}_o + \hat{d}_{\rm w}^\dagger)^\dagger (x\hat{d}_o + \hat{d}_{\rm w}^\dagger) \rangle \geq 0$, where x is an arbitrary real-valued parameter.

[7] J. Eisert, Ph.D. thesis, University of Potsdam, 2001; G. Vidal and R. F. Werner, Phys. Rev. A **65**, 032314 (2002); M.B. Plenio, Phys. Rev. Lett. **95**, 090503 (2005).

[8] B. Schumacher, and M. A. Nielsen, Phys. Rev. A **54**, 2629 (1996); S. Lloyd, Phys. Rev. A **55**, 1613 (1997).

[9] S.-H. Tan, B. I. Erkmen, V. Giovannetti, S. Guha, S. Lloyd, L. Maccone, S. Pirandola, and J. H. Shapiro, Phys. Rev. Lett. **101,** 253601 (2008).

[10] S. Pirandola, G. Spedalieri, S. L. Braunstein, N. J. Cerf, and S. Lloyd, Phys. Rev. Lett. **113**, 140405 (2014).

[11] C. Weedbrook, S. Pirandola, R. García-Patrón, N. J. Cerf, T. C. Ralph, J. H. Shapiro, and S. Lloyd, Rev. Mod. Phys. **84,** 621 (2012).

[12] I. Devetak, and A. Winter, Proc. R. Soc. Lond. A **461**, 207 (2005).

[13] Note that the expression of the entropic function $h(x)$ is that for vacuum noise equal to 1/2. Our notation is different from that of Ref. [11], where the vacuum noise is equal to 1.

[14] R. García-Patrón, S. Pirandola, S. Lloyd, and J. H. Shapiro, Phys. Rev. Lett. **102**, 210501 (2009).

[15] S. Pirandola, R. García-Patrón, S. L. Braunstein, and S. Lloyd, Phys. Rev. Lett. **102**, 050503 (2009).

[16] K. Modi, A. Brodutch, H. Cable, T. Paterek, and V. Vedral, Rev. Mod. Phys. **84**, 1655 (2012).

[17] For continuous-wave operation with a t_m-sec-long measurement interval, the $\hat{N}_\eta$ measurement is realized by the photon-count difference between the two detectors over that measurement interval.

[18] S. Guha and B. I. Erkmen, Phys. Rev. A **80,** 052310 (2009).